Circle, sphere, and drop packings

Tomaso Aste
Laboratoire de Physique Théorique, Université Louis Pasteur, 3 rue de l'Université, 67084 Strasbourg, France and C.I.I.M., Università di Genova, Piazz. Kennedy Pad. D-16129 Genova, Italy
(Received 2 March 1995; revised manuscript received 24 October 1995)

We studied the geometrical and topological rules underlying the dispositions and the size distribution of nonoverlapping, polydisperse circle packings. We found that the size distribution of circles of radii R that densely cover a plane follows the power law $N(R) \propto R^{-\alpha}$. We obtained an approximate expression that relates the exponent α to the average coordination number and to the packing strategy. In the case of disordered packings (where the circles have random sizes and positions) we found the upper bound $\alpha_{\max} = 2$. The results that were obtained for circle packing were extended to packing of spheres and hyperspheres in spaces of arbitrary dimension D. We found that the size distribution of dense packed polydisperse D spheres, follows, as in the two-dimensional case, a power law, where the exponent α depends on the packing strategy. In particular, in the case of disordered packing, we obtained the upper bound $\alpha_{\max} = D$. Circle covering generated by computer simulations gives size distributions that are in agreement with these analytical predictions. Tin drops generated by vapor deposition on a hot substrate form breath figures where the drop-size distributions are power laws with exponent $\alpha \simeq 2$. We pointed out the similarity between these structures and the circle packings. Despite the complicated mechanism of formation of these structures, we showed that it is possible to describe the drop arrangements, the size distribution, and the evolution at constant coverage, in terms of maximum packing of circles regulated by coalescence.

PACS number(s): 82.20.Wt, 02.40.−k

I. INTRODUCTION

A plane is not very efficiently covered with circles, but circle covering is a good model system for the study of the formation and evolution of many natural and artificial systems, such as granular materials [1, 2], island formation in metal films [3, 4], segregation problems [5], plate tectonics and turbulence [6, 7], and focal arrangement in smetic liquid crystals [8, 9]. One interesting problem related to packing circles is to find the size distribution that efficiently leads to the densest covering compatible with the packing strategy. In some particular cases, such as the Apollonian covering [10] (where the circles are packed all tangent to each other following a defined sequence), analytical and numerical solutions are available in the literature [6, 7, 11, 12]. In this paper the problem is discussed in the general case of disordered packing (or "osculatory" packing), where the circles are set with random sizes and positions. The motivation of this work is to understand the basic mechanisms which underlie the morphogenesis of breath figures [13–18]. Water which condenses on a glass form a densely-packed system of droplets known as a breath figure. The formation of the droplet system is regulated by two basic mechanisms: the *independent growth* of a drop supported by condensation and the melting of two or more drops in a *coalescence* phenomenon. These two mechanisms lead to systems with a wide range of drop sizes. The distribution is characterized by rather uniform drop sizes in the region of large radii (drops which are grown from the originally nucleated drops through a chain of independent growth and coalescence) and a power law in the region of small radii (drops which are generated by renucleation on the surface liberated by coalescence). The formation of these structures is an extremely complicated dynamical process. The point of view here adopted is that the system morphogenesis is mainly driven by the geometrical constraints which regulate the drop packing.

Two-dimensional structures generated by packing circles (or by packing other isotropic natural objects like dewdrops on a glass), have some properties which are independent of the specific formation mechanism. The main similarities can be schematized in the following three points: (i) a wide range in the sizes; (ii) a scale invariance in the packing arrangement; (iii) a power law in the size distribution [$N(R) \propto R^{-\alpha}$]. Let us briefly discuss the possible physical origin of these three similarities.

(i) A wide range in the particle sizes is a necessary condition to reach dense packing. For example, the packing of circles with equal radii R_0 has a maximum density of 0.907. The density can be raised to $\rho = 0.95$ by filling the interstitial spaces with circles of sizes $R_1 = R_0/6.4$. Another increment to $\rho = 0.97$ requires interstitial radii equal to $R_2 = R_0/15.9$. In general, the density can be increased up to any value $\rho < 1$, but this requires the utilization of interstitial circles with dimensions which rapidly decrease.

(ii) Consider a procedure where dense circle packing is generated by filling the interstitial spaces with circles of the maximum size compatible with the condition of nonoverlapping. (Note that, if the maximum radius is fixed, this procedure generates structures which minimize the surface extension at fixed covered area.) In this procedure the only relevant metric parameter is the ratio between the external radii of the circles that generate an

interstice and the internal radius of the circle that fill this interstice. For example, in the Apollonian case, this ratio tends to the value $x \simeq 2.9$. In general, x tends to a constant value that is related to the packing strategy. It is straightforward to see that packing characterized by constant values of x is scale invariant.

(iii) The number of circles introduced at any covering step increases following a geometrical progression. For example, in the Apollonian packing, if one starts with four circles in contact, at the first covering step one has three interstitial spaces to fill by circles, at the second step the interstices to fill are 9, at the third step this number is 27, and, at the νth it is 3^ν. In the general case, the number of circles introduced at any stage grows as a geometrical progression a^ν. By associating this increment in the number of interstitial circles with the condition of scale invariance, one obtains a size distribution that follows the law $N(R) \propto R^{-\alpha}$, where the coefficient α depends on the packing strategy.

In this paper we obtain an approximate expression that relates the exponent α to the local topological properties of the circle packing and to the packing strategy. The limiting value of such a coefficient in the case of disordered maximum packing has been found equal to 2.

Simple computer simulations of disordered circle covering have been performed. The results, presented in Sec. IV, confirm the theoretical predictions: the circle-size distribution follows a power law with exponent $\alpha \simeq 2$.

The size distribution of tin droplets condensed on a hot, flat surface has been experimentally studied [19–23]. In Sec. V, the experimental data are interpreted in terms of maximum circle packing. Through this point of view it is possible to give a simple explanation of some statistical and dynamical characteristics of these systems. In particular, the drop-size distribution, the coverage, and the self-similar evolution at constant coverage have been interpreted in the framework of maximum packing of drops regulated by coalescence.

II. TOPOLOGICAL AND GEOMETRICAL RULES IN PACKING

Consider a plane densely covered by circles placed at random following the only constraint of nonoverlapping. Consider the Dodds network [24] constituted by the edges that connect the centers of circles in contact (see Fig. 1). Such a network has a number of vertices (in the following indicated by V) equal to the number of circles. The vertex connectivity ($\langle z \rangle$) is the average number of neighbors in contact with a circle. The other network parameters (in particular the number of edges E and the number of faces F) are given, in term of V and $\langle z \rangle$, by the relation [25]

$$\langle z \rangle V = 2E \tag{1}$$

(any vertex is surrounded by $\langle z \rangle$ edges and any edge is bounded by two vertices), and by Euler's formula

$$V - E + F = \chi \quad , \tag{2}$$

where χ is the Euler-Poincaré characteristic and takes the value of 1 for a Euclidean plane. Note that Eq. (1) holds only if in the network there are no insulated vertices. This condition is generally satisfied in densely packed systems.

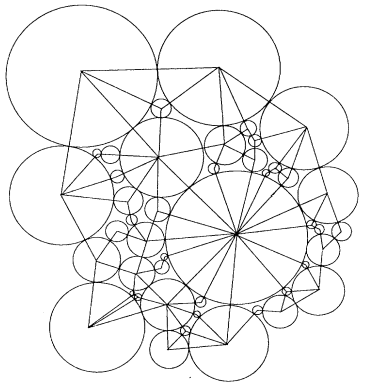

FIG. 1. The Dodds network generated by connecting the centers of circles mutually in contact.

The combination of Eqs. (1) and (2) leads to a useful relation between the number of circles V and the number of interstitial spaces between the circles [which is equal to the number of faces (F) of the Dodds network]. We have

$$F = \left(\frac{\langle z \rangle}{2} - 1 \right) V + \chi \quad . \tag{3}$$

Note that at the point $\langle z \rangle = 2$ the interstitial spaces between circles become connected ($F = \chi = 1$, in the Euclidean plane) and, consequently, the network becomes unconnected. This is the percolation threshold in two dimensions. For the purposes of the present paper the opposite limit is interesting (since we are investigating the properties of dense packing). From a topological point of view, the densest circle packing is characterized by circles which are all in contact among neighbors. In such a packing the interstices between circles are all closed and surrounded by three circles. In this case, the identity $3F = 2E$ holds (any face has three edges and any edge divides two faces) and the vertex connectivity reach its maximum value $\langle z \rangle_{\max} = 6(1 - \frac{\chi}{V})$. In general, less dense packings are characterized by lower value in the vertex connectivity (for example a typical connectivity for disordered packing of binary and polydisperse mixtures of circles is $\langle z \rangle \simeq 3.75$ [25]).

A. Apollonian covering

An example of topologically densest circle packing is the Apollonian covering. In such a packing, any circle is in contact with three surrounding circles. A well known formula (*the kiss precise* [10, 26]) gives a relation between the curvatures $\epsilon_i = 1/R_i$ of the four "kissing" circles of radii R_i, $i = 1, ..., 4$

$$2(\epsilon_1^2 + \epsilon_2^2 + \epsilon_3^2 + \epsilon_4^2) = (\epsilon_1 + \epsilon_2 + \epsilon_3 + \epsilon_4)^2 \quad . \tag{4}$$

Following Coxeter [27], one can consider the case in which the curvatures belong to a geometric progression $\epsilon_\nu = x^\nu \epsilon_0$, where x is the ratio of the progression. Substituting into (4) one gets a sixth order equation in x with only one real root bigger than 1: $x \simeq 2.89$. In general, similar values for the ratio $\epsilon_{\nu+1}/\epsilon_\nu$ are characteristic of several covering sequences. For example, a value slightly less than 2.9 is the ratio at which the loxodromic spiral sequence converges [27]. These values correspond to particular sequences selected from the whole covering set. The analytical evaluation of an average value of x corresponding to the complete set of covering sequences is still an open problem [28].

The Apollonian covering is a well-defined problem and constitutes an excellent example of circle covering. On the other hand, the aim of this work is the study of natural systems which have a higher degree of randomness in the packing strategy.

B. Disordered covering

Let us consider a covering procedure that utilizes nonoverlapping circles with sizes distributed between two radii $R_{\max}$ and $R_{\min}$. Such a procedure starts filling the available space with the circles of higher radius $R_0 = R_{\max}$. Once the interstitial spaces between these circles become too small to contain circles with the maximum radius the procedure reduces the radius of the new circles to insert $R_1 = R_0/x$. The filling continues iterating this process gradually reducing the radii $R_\nu = x^{-\nu} R_0$ in order to insert circles of biggest radius compatible with the interstitial size. Placing the centers in appropriate positions, this procedure generates the Apollonian sequences of tangent circles discussed in the previous paragraph. More generally, one can study a disordered covering where the circles are placed with the centers at random. Unlike the Apollonian case, in this covering the circles are not all tangent. In the Apollonian covering the interstitial space is always generated by three circles all in contact with each other. In the disordered case, the same three circles are—in general—not all tangent and the interstitial space is bigger. It follows that, in this case, the interstitial space can be filled with circles of bigger sizes than in the Apollonian case. Consequently, the ratio between the radii of the circles that form the boundary of an interstice and the circle that fills this interstice is lower in the disordered covering than in the Apollonian case. Thus the value $x \simeq 2.9$ suggested as a limit of the ratio $\epsilon_{\nu+1}/\epsilon_\nu$ in the Apollonian sequence of tangent circle, represents, for the disordered case, an upper limit.

It is now interesting to investigate the lower limit for x. This limit can be achieved by imposing the condition that the sum of the areas of all the circles introduced with the covering procedure converges to a finite value (which must be lower than the total area to cover).

Consider, as before, a covering characterized by a sequence of radii in the geometrical progression $\epsilon_\nu^{-1} = R_\nu = x^{-\nu} R_0$. The number of interstitial circles introduced at any stage ν is equal to the number of interstices of the system at that stage. This number is given by Eq. (3) as

$$F_\nu = \left(\frac{\langle z \rangle}{2} - 1\right) V_\nu + \chi \quad , \tag{5}$$

where V_ν is the number of circles at the stage ν.

The covering goes on, filling these interstices with F_ν new circles of radius $R_{\nu+1}$. The number of interstices at the stage $\nu + 1$ is then

$$F_{\nu+1} = \left(\frac{\langle z \rangle}{2} - 1\right)(V_\nu + F_\nu) + \chi \quad . \tag{6}$$

Substituting the value of V_ν given by Eq. (5) into (6), one gets

$$F_{\nu+1} = \left(\frac{\langle z \rangle}{2}\right) F_\nu \quad , \tag{7}$$

which yields

$$F_\nu = \left(\frac{\langle z \rangle}{2}\right)^\nu F_0 \quad . \tag{8}$$

The total area covered by the circles at the stage ν is given by the sum over the areas covered at any stage until ν:

$$\begin{aligned} A_\nu &= \pi \left(V_0 R_0^2 + \sum_{i=1}^{\nu} F_i R_i^2 \right) \\ &= \pi R_0^2 \left[V_0 + F_0 \frac{\langle z \rangle}{2x^2} \sum_{i=0}^{\nu} \left(\frac{\langle z \rangle}{2x^2} \right)^i \right] \quad . \end{aligned} \tag{9}$$

When $\nu \to \infty$, this sum converge to a finite number only if $\langle z \rangle/(2x^2) < 1$. This condition gives the lower limit for the sequence ratio

$$x > \sqrt{\frac{\langle z \rangle}{2}} \quad . \tag{10}$$

Note that Eq. (8) has been obtained supposing the coordination number $\langle z \rangle$ and the ratio x to be constant at any covering stage. This is not in general true. (The value of $\langle z \rangle$ is fixed and equal to 6 in the Apollonian covering of an infinite Euclidean plane but not in general. Moreover, also in this particular case, the ratio x is constant only in the asymptotic limit.) It should be noted that the convergence condition for the total area constrains only the asymptotic values of x and $\langle z \rangle$. [It is straightforward to see that, in the Apollonian case, Eq. (10) is satisfied by the asymptotic values ($x \simeq 2.9$ and $\langle z \rangle = 6$).] In the asymptotic limit, the covering procedure is in general scale invariant, as the only important metric parameter is the ratio between the sizes of the circles that generate an interstice and the size of the circle that fills this interstice. In this asymptotic limit the parameters $\langle z \rangle$ and x are related only to the covering strategy and are independent of the specific stage ν. The inequality (10) constrains these asymptotic parameters.

III. CIRCLE-SIZE DISTRIBUTION

The circle-size distribution $[N(R)]$ is related to the value of x and to the number of cells introduced at any

covering step. By associating the relation $R_\nu = R_0 x^{-\nu}$ with Eq. (8), one gets

$$N(R_\nu) = N_0 \left(\frac{R_0}{R_\nu}\right)^\alpha \quad , \tag{11}$$

where the exponent is

$$\alpha = \frac{\ln\left(\frac{\langle z\rangle}{2}\right)}{\ln x} \quad . \tag{12}$$

Above we pointed out that the value of $\langle z\rangle$ is associated with the packing strategy: it is equal to 6 in the Apollonian case, whereas in the disordered covering it tends gradually to asymptotic values lower than or equal to 6. In the previous paragraph we discussed the bounds on the value of x. Substituting the lower bound given by Eq. (10) one gets the upper limit for the exponent α,

$$\alpha < \frac{\ln\left(\frac{\langle z\rangle}{2}\right)}{\ln\sqrt{\frac{\langle z\rangle}{2}}} = 2 = \alpha_{\max} \quad , \tag{13}$$

which is independent of $\langle z\rangle$.

We discussed above that the upper bound of x is associated with the Apollonian covering. In this case we have $x \simeq 2.9$ and $\langle z\rangle = 6$ which leads to $\alpha = 1.03$.

The Hausdorff-Basicovitch fractal dimension of the packing can be directly derived from the size distribution [6]; one finds $d_f = \alpha$. The analytical determination of d_f is a challenging problem of surprising difficulty. Only bounds are known, $1.300\,197 < d_f < 1.314\,534$ [6, 11]. The value here derived is quite far from the two exact bounds and from the value $d_f = 1.305\,684$ obtained by numerical calculations. It should be noted that our relation (12) is an approximate solution and that the value of $x = 2.9$ that we assumed in (13) is only an estimation valid for a particular subset of all the possible covering sequences. On the other hand, values of $1 \le \alpha \le 2$ are in agreement with two exactly solvable models discussed in Appendix B [9]. In these particular cases (where x is constant) one has $d_f = \alpha = 1$ and $d_f = \alpha = 1.585$.

Note that, in the literature (for example, [6, 11]) the size distributions are discussed in the continuous limit. Here $N(R_\nu)$ is a discrete distribution stating the number of circles with radius R_ν. In the continuum limit, $N(R_\nu)$ corresponds to the integral of the continuous distribution $n(R)$ evaluated between $R_{\nu+1}$ and R_ν. From Eq. (11) and using the identity $R_{\nu+1} = R_\nu/x$, one obtains $n(R) = CR^{-\alpha-1}$ with $C = \alpha N_0 R_0^\alpha/(x^\alpha - 1)$ [$n(R)dR$ being the number of circles with radius between R and $R + dR$].

A. Generalization to arbitrary dimensions

It is possible to extend the results obtained in the previous paragraph to spaces of any dimension. The calculus can be done following the same principal points utilized in the two-dimensional case, extending the notions developed for the circles to D spheres.

Consider the network obtained by connecting with edges the centers of all the D spheres mutually in contact. The number of vertices (V) of such a network is equal to the number of D spheres. The number of cells (in the following indicated by C) is given by the relation

$$C = \frac{n_{D,0}}{n_{0,D}} V \quad , \tag{14}$$

where $n_{D,0}$ is the mean number of D cells incident on a vertex and $n_{0,D}$ is the mean number of vertices bounding a D cell. In two dimensions, the incidence number $n_{2,0}$ is the vertex connectivity $\langle z\rangle$ and $n_{0,2}$ is the mean number of edges per face $\langle n\rangle$. In a planar network these two parameters are connected through the relation

$$\langle n\rangle = \frac{2\langle z\rangle}{(\langle z\rangle - 2 + \frac{2\chi}{V})} \quad . \tag{15}$$

Substituting this relation into (14) one gets immediately Eq. (5). For $D > 2$, $n_{D,0}$ and $n_{0,D}$ are, in general, independent, free parameters related to the network peculiarities. [For example, a particular case is the topological densest packing where any D sphere is in contact with all the surrounding spheres. In this case any interstitial space is bounded by $D+1$ D spheres. In such a packing the network is made only by hypertetrahedra and one has $n_{0,D} = D+1$ (any hypertetrahedron has $D+1$ vertices). On the other hand, the incidence number $n_{D,0}$ is, also in this particular case, a free parameter which depends on the network characteristic. For $D = 3$, the maximum value of $n_{3,0}$ for the packing of equal spheres is 22.6 [29]. By filling the interstices with smaller sized spheres this number is reduced up to the lower limit of 12.]

Consider the system at the covering stage ν. At this stage, V_ν D spheres are packed. The number of interstices between them is $C_\nu = (n_{D,0}/n_{0,D})V_\nu$. At the following stage $\nu + 1$, these interstices are filled with C_ν D spheres. Thus the total number of D spheres in the system becomes

$$V_{\nu+1} = V_\nu + C_\nu = \left(1 + \frac{n_{D,0}}{n_{0,D}}\right) V_\nu \quad . \tag{16}$$

Consequently the number of interstices is

$$C_{\nu+1} = \left(1 + \frac{n_{D,0}}{n_{0,D}}\right) C_\nu \quad , \tag{17}$$

which gives

$$C_\nu = \left(1 + \frac{n_{D,0}}{n_{0,D}}\right)^\nu C_0 \quad . \tag{18}$$

This equation generalizes Eq. (8).

The covering procedure should be scaling invariant: in the covering strategy all that is important is the ratio between the radii of the D spheres that bound the interstitial space and the radius of the sphere that fills this interstice. The only important metric parameter that characterizes the covering procedure is the ratio $x = R_\nu/R_{\nu+1}$. A limiting value for x can be obtained—as in the two-dimensional (2D) case—by requiring that the sum over the volumes introduced with the covering procedure con-

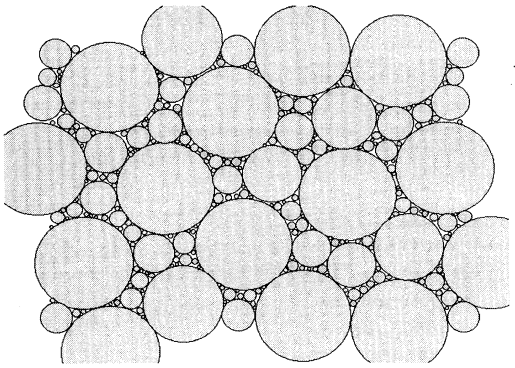

FIG. 2. Computer generated circle covering.

verges to a finite value:

$$\lim_{\nu\to\infty}\sum_{i=0}^{\nu} C_i R_i^D = C_0 R_0^D \lim_{\nu\to\infty}\sum_{i=0}^{\nu}\left(\frac{1+\frac{n_{D,0}}{n_{0,D}}}{x^D}\right)^i = A \quad . \tag{19}$$

This condition gives a lower limit for x:

$$x > \left(1+\frac{n_{D,0}}{n_{0,D}}\right)^{1/D} \quad . \tag{20}$$

An upper limit for x can be calculated by solving the algebraic equation obtained by substituting ϵ_ν with $\epsilon_\nu = x^\nu$ into the generalization to any D of Eq. (4) [30]. (For example, one obtains $x \simeq 1.88$ for $D = 3$, $x \simeq 1.55$ for $D = 4$, $x \simeq 1.39$ for $D = 5$, $x \simeq 1.30$ for $D = 6$, and $x = 1$ for $D \to \infty$.)

The size distribution can be obtained by associating Eq. (18) with the condition $R_{\nu+1}/R_\nu = x$. One has

$$N(R_\nu) = N_0\left(\frac{R_0}{R_\nu}\right)^\alpha \quad , \tag{21}$$

where the coefficient is

$$\alpha = \frac{\ln\left(1+\frac{n_{D,0}}{n_{0,D}}\right)}{\ln x} \quad . \tag{22}$$

By substituting the lower limit of x [maximum packing, Eq. (20)] one obtains the upper bound for the exponent $\alpha_{\max} = D$. The lower bound for α can be calculated by substituting into Eq. (22) the maximum value of x (which corresponds to the Apollonian case) and the minimum value of the coefficient $n_{D,0}/n_{0,D}$. This last parameter depends on the packing strategy. For $D = 3$, the Apollonian packing has $n_{0,D} = 4$, $n_{D,0} > 12$, and $x \simeq 1.88$. In this case, one gets the limit of $\alpha \simeq 2.2$.

The two models, discussed in Appendix B, can easily be extended to the 3D case, one obtains $\alpha = 1.26$ and $\alpha = 2$ for the hexagonal and triangular models, respectively.

IV. COMPUTER SIMULATIONS

The covering procedure starts positioning the circles with maximum radius $R_0 = R_{\max}$. The position of the center of each circle is chosen at random. A new circle is added to the system only if it is nonoverlapping with any other preexisting circle, otherwise another random position is chosen. This first step ends when all the interstitial spaces between circles have sizes smaller than the circle diameter and thus new circles with radius $R_{\max}$ cannot be positioned any more. At the second step, the radius of the new circles is reduced to $R_1 = R_0/x$, the centers are chosen at random, and a new circle is placed only if it is nonoverlapping with any other preexisting circle. The procedure continues gradually reducing the sizes of the circles to place once the interstitial spaces become too small to contain new circles. No shifting or rearrangement is performed once a circle has been positioned. The procedure ends, after a finite number of steps, at the lowest radius $R_{\min}$.

In Fig. 2 is shown a typical structure obtained by using this procedure. Figures 3(a) and 3(b) show the circle-size distribution in normal and double logarithmic scale, for two simulations. The data have been obtained

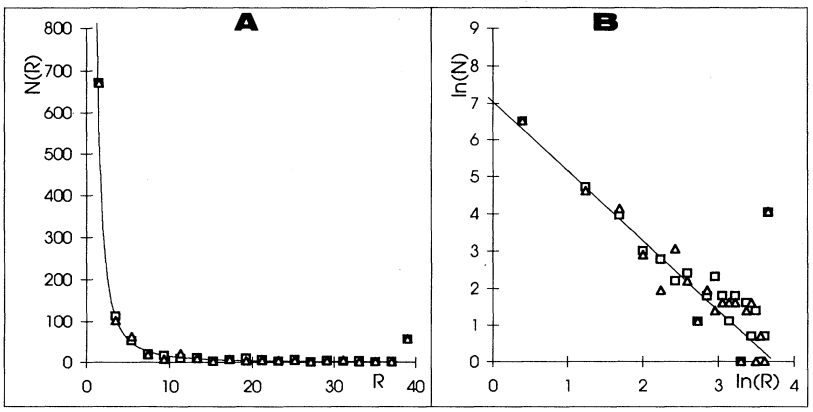

FIG. 3. Size distributions of two computer generated circle coverings. (a) Normal scale. (b) Double logarithmic scale. The full line is the average best fit.

covering a rectangle of 600 × 450 pixels with periodic boundary conditions. The maximum radius was R_{max} = 45 pixels and the minimum was R_{min} = 1.5 pixels. In accordance with the covering procedure, the circle size has been decreased between R_{max} and R_{min} in 50 finite steps. In the simulations reported in Fig. 3, the total number of circles was respectively equal to 995 (squares) and 987 (triangles).

The circle-size distribution is characterized by one peak at the maximum radius and by a fast increment towards the minimum radius. The linear trend of the distribution, in the region of small radii ($R < R_{max}/5$), shown in the double logarithmic scale [Fig. 3(b)], suggests a power law $N(R) \propto R^{-\alpha}$. The best-fit estimation for the exponent gives $\alpha = 1.84 \pm 0.16$ (squares) and $\alpha = 1.92 \pm 0.19$ (triangles), with confidence factors respectively equal to 93% and 92%.

A power law for the size distribution was analytically predicted in the previous paragraphs and in Appendix A. The best-fit values of the exponents α are in good agreement with the theoretical predictions for the case of disordered maximum circle packing.

V. STRUCTURES FORMED BY CONDENSED TIN DROPLETS

Figure 4 is a scanning electron microscope (SEM) micrograph of Sn drops condensed on a hot, flat alumina substrate. The system was prepared by evaporating the tin in high vacuum on a substrate heated at a temperature higher than the tin melting point [31, 23]. After cooling at room temperature, one has a stable system of packed tin drops. The size distribution of such a system was studied using SEM micrographs of magnifications 10 000× and 20 000×. The micrographs were digitized with a scanner. On each image an internal rectangular perimeter was defined and the drops inside and on the bound perimeter were encircled with circles of the same size as the surface occupied by the drop. The size distribution of these circles was studied. The boundary effects were taken into account by counting 1/2 the circles crossing an edge of the perimeter and 1/4 of the circles containing a vertex of the bound perimeter. In Fig. 5 the sizes distributions for three different samples are reported in normal and double logarithmic scales. The three samples were deposited respectively with 2.5 (triangles), 2.8 (squares), and 3.2 g/m^2 (diamonds). The biggest drops have sizes of about 1000 nm, whereas the smallest (measurable) drop sizes are 50 nm. The number of drops encircled per each micrograph was about 2000–2500. The distribution is characterized by rather uniform drop sizes in the region of large radii and by a fast increment, such as a power law, towards the smallest radii.

Typically, one drop nucleates on a preferential center and grows supported by condensation. This independent growth stops when the drop touches another surrounding drop. At this point, the two drops melt together and the new drop formed eventually melts with other surrounding drops in a chain of coalescence events. The coalescence leads to a new drop with volume equal to the sum of the volumes involved in the coalescence phenomenon. This new drop occupies a surface smaller than the sum of the surfaces occupied by the original drops. It follows that the coalescence mechanism liberates space on the substrate. On this surface the nucleation, growth, and coa-

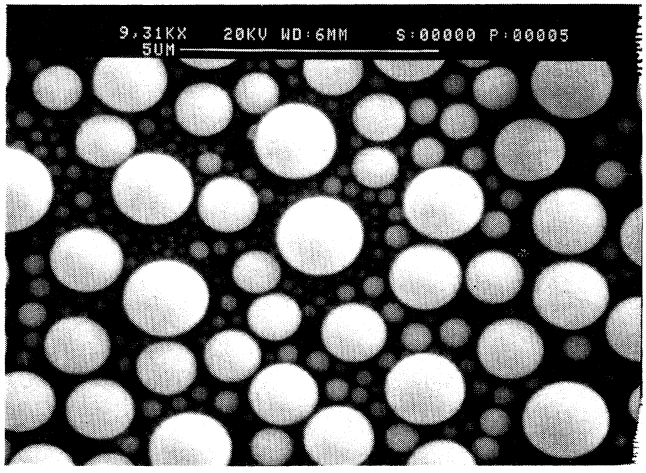

FIG. 4. SEM micrograph of a breath figure generated by tin drops deposited on a hot alumina substrate.

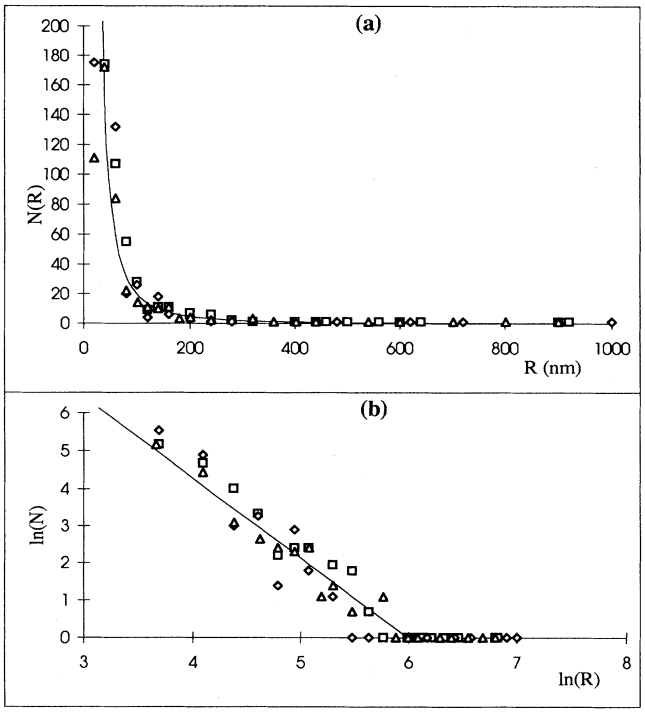

FIG. 5. Size distribution of the tin drop diameters for three different samples. (a) Normal scale; (b) double logarithmic scale. In ordinates, $N(R)$ is the number of drops per μm^2. The full line is the average best fit.

lescence phenomena can start again. The final structure is therefore a consequence of a very complicated process which involves many-body phenomena [13]. Nevertheless the formation of the final structure can be investigated adopting a simple point of view.

The system of quenched drops shown in Fig. 4 is apparently similar to the systems studied, analytically and numerically, in the previous paragraphs. This similarity is not only apparent: the nucleation, growth, and coalescence mechanism leads to systems where the drops occupy the maximum possible surface and have the biggest sizes compatible with the coalescence that prevents the drops overlapping. The system evolves through self-similar configurations where the size distribution is, at any time, the maximum packing distribution.

The similarity between these two systems is confirmed by the drop-size distribution: in the region of small radii the distribution follows a power law $N(R) \propto R^{-\alpha}$ with exponent $\alpha \simeq 2$. The best fit gives $\alpha = 1.96 \pm 0.13$ (triangles in Fig. 5), $\alpha = 2.05 \pm 0.11$ (squares), and $\alpha = 2.1 \pm 0.23$ (diamonds), with confidence factors respectively equal to 94%, 95%, and 87%. These values are in accordance with the analytical predictions and strongly suggest that the system morphogenesis is ruled by the mechanism of the maximum circle packing.

In the region of large radii ($R \simeq R_{\max} > 500$ nm) the drops have rather uniform sizes. This region of uniform sizes is the memory of the first stage of the deposition where the drops grow independently. Indeed, in this stage the relative volumes of the drops are proportional to the sizes of the Voronoi cell constructed around the drop centers [32], and a rather uniform distribution is expected. In Fig. 5 this uniformity at $R \simeq R_{\max}$ is not particularly manifest since the number of drops in this region is small in comparison with the number of small drops (for example, in a sample deposited with about 3 g/m^2, one has about ten drops per μm^2 of about 0.1 μm and one drop per μm^2 of 1 μm). Despite the fact that their number is little, the big drops cover a large amount of surface and contain the main part of the volume deposited (using the same example reported above, it is straightforward to see that the big drops cover an area 10 times larger and occupy a volume 100 times larger than the small drops). Note that a peak at $R_{\max}$ is present also in the computer simulations. A deviation from the maximum packing law in the region close to $R_{\max}$ is not in contradiction with the theoretical predictions. The analytical result $N(R) \propto 1/R^{\alpha}$ concerns only the asymptotic limit of the distribution ($\nu \to \infty$, i.e., $R/R_{\max} \to 0$) where the system is supposed to be scale invariant.

Studies reported in the literature [13–17, 33, 18, 34] show that the system of condensed drops evolves in time by increasing the drop sizes, decreasing the drop number, and maintaining the coverage constant. In the systems of tin drops studied here, the coverage has been experimentally found in the range 60% to 65% [20, 23]. A small value of the coverage (typically in breath figures it is equal to about 55% [33]) is a consequence of coalescence which continuously liberates space. Consider a configuration of three external drops of radius R_0 and one interstitial drop of radius R_1. The collapse of these four drops into one through coalescence liberates a certain amount of surface. The fraction of area liberated [(area occupied by the drops after coalescence)/(area occupied before coalescence)] is slightly dependent on the packing strategy. It is equal to 32% if the four drops are all "kissing" each other and equal to 35% in the case of disordered maximum packing ($R_0/R_1 = x \simeq \sqrt{3}$). The presence of other interstitial drops that participate in the coalescence phenomenon reduces the previous values within 1%. Starting with an initial—hypothetical—coverage of 100%, the coalescence reduces the coverage to 68% and 65% in the two cases discussed above. These values are close to the coverage experimentally observed. Note that these values are scale invariant and depend only on the local configurations of drop (i.e., on the packing strategy). The scale invariance implies that the fraction of area liberated by coalescence is independent of the drop radii (i.e., independent of the amount of tin deposited) and thus constant during the deposition.

VI. CONCLUSIONS

Circle covering is a good model system for many two-dimensional natural cellular systems where a plane is filled in the most efficient way compatible with the cell shapes and sizes. It has been found (Secs. II and III and Appendix A) that polydisperse circles packed in a dense way have a size distribution that follows the general law $N(R) \propto R^{-\alpha}$. This distribution is a consequence of the scale invariance in the packing strategy. The range of variability of the exponent has been calculated. We have obtained a maximum value of $\alpha_{\max} = 2$ for the general disordered case, where the circles are arranged at random following the only constraint of nonoverlapping. The minimum value has been estimated as $\alpha_{\min} \simeq 1$ and corresponds to an approximate solution for the Apollonian packing (Secs. II A and III), and to an exact solution for the "hexagonal" filling model (Appendix B).

These results, obtained for two-dimensional circle packing, have been extended to packing of spheres in spaces of arbitrary dimension (Sec. III A). We found that, in D-dimensional spaces, the size distribution of densely packed D spheres follows—as in 2D—power law $N(R) \propto R^{-\alpha}$. In this generalized case, the maximum value of the exponent is $\alpha_{\max} = D$ and is associated with disordered packing. The minimum value is associated with the packing of tangent D spheres. For $D = 3$, this value has been estimated equal to $\alpha = 2.2$ for the Apollonian case, whereas for the hexagonal filling model we found $\alpha = 1.26$.

Computer simulations of two-dimensional circle packing confirm the analytical predictions: in the disordered case the size distribution follows a power law with exponent $\alpha \simeq 2$ (see Sec. IV).

The formation of breath figures has been interpreted in terms of circle packing regulated by coalescence (Sec. V). The mechanism of formation of these figures is very complicated since it is a dynamic system where the evolution involves many-body phenomena. On the other hand, the structures formed by the drops instant by instant

have strong similarities with the structures generated by packing circles. In particular, the size distribution in the region of small radii follows the same power law as the disordered, dense circle packing with exponent $\alpha \simeq 2$. The coverage, evaluated through the fraction of area liberated by coalescence in a system of drops that follows the maximum packing distribution, is in agreement with the experimental observations.

ACKNOWLEDGMENTS

The author wishes to thank Rodolfo Botter for the help given in the sample preparation, the microstructural characterization, and for useful discussions. A special thanks to Professor Dario Beruto for the useful discussion and suggestions. The author thanks F. Saya and P. Pozzolini for the measurements of the drop-size distributions. Finally, the author thanks Nicolas Rivier for useful discussions.

APPENDIX A: SIZE DISTRIBUTION AND COVERING STRATEGIES

In the second and third section we found that the size distribution of densely packed circles follows a power law [Eq. (11)] where the exponent α is related to the topological properties of the Dodds network and to the parameter x [Eq. (12)]. This is a general result where the only *a priori* hypothesis is the existence of a Dodds network with convex cells (this condition can be considered as the definition of dense packing). In this appendix we generalize these results using an approach which does not need the definition of the Dodds network.

Consider a covering procedure which fills the available space with nonoverlapping circles starting from the circles of bigger sizes $R_{\max}$ and then gradually reducing the sizes $R_\nu < R_{\max}$ in order to fill the interstitial spaces. The number of circles introduced at any covering step and the relative sizes depend on the covering procedure. In the second section we pointed out that the scaling condition implies that the number of circles inserted at any covering step grows as a geometrical progression $N_\nu \propto a^\nu$ and the size of the circles decreases as a geometrical progression $R_\nu \propto R_0/x^\nu$. As a consequence the size distribution results as a power law $N(R_\nu) \propto R_\nu^{-\alpha}$ with exponent

$$\alpha = \frac{\ln a}{\ln x} . \tag{A1}$$

In the case of dense packing (i.e., when it is possible to define a Dodds network with convex cells) we found $a = \langle z \rangle/2$ [Eq. (22)] and the bound $x > \sqrt{\langle z \rangle/2}$ [Eq. (10)].

More generally one can construct the Delaunay triangulation with the center of the circles as vertices. This triangulation is always well defined and (for an infinite system) the average connectivity is $\langle z \rangle = 6$. Different packing strategies differentiate the number, the sizes, and the positions of the new vertices (i.e., the new circles) to insert. From a topological point of view, there are only two positions where the center of the new circles can be placed: inside a triangle or on an edge (the center on a vertex is forbidden by the condition of nonoverlapping). Suppose that the packing procedure places a new circle with probability p inside a given triangle and with probability q on a given edge of the Delaunay triangulation. If V_ν is the number of vertices (i.e., of circles) at the covering stage ν, it is easy to prove (following the same arguments as in Sec. II) that at the next stage this number is

$$V_{\nu+1} = (1 + 2p + 3q)V_\nu \quad . \tag{A2}$$

From relation (A2) it follows immediately that the number of circles grows as a geometrical progression ($N_\nu = V_\nu \propto a^\nu$) with coefficient $a = (1 + 2p + 3q)$.

The argument used in Sec. II to find the lower bound on the parameter x [Eq. (10)] can be directly extended to the present case. One gets $x > \sqrt{a}$, which, substituted in (A1), gives the upper limit $\alpha_{\max} = 2$.

The Apollonian covering is a particular example of the covering procedure here discussed. In this case one has $p = 1$, $q = 0$, and $x \simeq 2.9$, which gives $\alpha \simeq 1$.

APPENDIX B: HEXAGONAL AND TRIANGULAR FILLING MODELS

Following the work of Bidaux *et al.* [9], let us describe two simple circle-covering problems where the exponent α can be calculated exactly. Originally these models were proposed as simplified geometrical problems to estimate two bounds for the fractal dimension in Apollonian packing. In the present work these two models are presented as good examples of circle covering which do not necessarily correspond to approximations of the Apollonian case.

Let us start with one triangle (not necessarily equilateral). In the first model (*triangular*), one inserts a new triangle with vertices at the mean points of the edges of the original triangle. In this way the original triangle is divided into four identical triangles which are similar to the original. Then one inserts a circle inside the central triangle and iterates the procedure on the three external triangles. At the beginning one starts with one circle, at the first step one inserts three new circles, and at the νth step the number of new circles inserted is 3^ν. The parameter a (see Appendix A) is then equal to 3. The ratio x can be easily derived by observing that the triangles are all similar and that at each step of the sequence the sizes of the edges are reduced by a factor of 2. Consequently one has $x = 2$. Substituting the parameters a and x into Eq. (A1) one gets the exponent $\alpha = \ln 3/\ln 2 \simeq 1.58$.

In the second model (*hexagonal*) one inscribes first a hexagon with vertices which divide in three equal parts the edges of the original triangle. Then a circle is inscribed inside the hexagon and the procedure is iterated on the three remaining external triangles. As before one obtains $a = 3$, whereas the scale factor is $x = 3$. By substituting into Eq. (A1) we get the exponent $\alpha = 1$.

Note that, if one uses equilateral triangles, the coverage θ [(area covered by the circles)/(area of the original triangle)] can be calculated exactly. One has $\theta = \pi/(3\sqrt{3}) \simeq 0.6$ for the triangular model and $\theta = \pi/(2\sqrt{3}) \simeq 0.9$ for the hexagonal. These values can be increased by inserting new triangles in the free interstices between the circles and iterating the procedure.

[1] See, for example, *Physics of Granular Media*, edited by D. Bideau and J. Dodds (Nova Science, New York, 1991).
[2] E. Guyon, S. Roux, A. Hansen, D. Bideau, J. P. Troadec, and H. Crapo, Rep. Prog. Phys. **53**, 373 (1990).
[3] J. A. Blackman and A. Wilding, Europhys. Lett. **16**, 115 (1991).
[4] J. A. Blackman and A. Marshall, J. Phys. A **27**, 725 (1994).
[5] J. P. Troadec, A. Gervois, C. Annic, and J. Lemaitre, J. Phys. (France) I **4**, 1121 (1994).
[6] H. J. Hermann, G. Mantica, and D. Bessis, Phys. Rev. Lett. **65**, 3223 (1990).
[7] S. S. Manna and H. J. Hermann, J. Phys. A **24**, L481 (1990).
[8] Y. Bouligand, J. Phys. (Paris) **33**, 525 (1972).
[9] R. Bidaux, N. Boccara, G. Sarma, L. de Seze, P. G. de Gennes, and O. Parodi, J. Phys. (Paris) **34**, 661 (1973).
[10] H. S. M. Coxeter, *Introduction to Geometry* (J. Wiley and Sons, New York, 1961).
[11] D. W. Boyd, Mathematica **20**, 170 (1973).
[12] B. B. Mandelbrot, *The Fractal Geometry of Nature* (W. H. Freeman and Company, San Francisco, 1982), Chap. 18.
[13] D. Beysens and M. Knobler, Phys. Rev. Lett. **57**, 1433 (1986).
[14] B. J. Briscoe and K. P. Galvin, Phys. Rev. A **43**, 1906 (1990).
[15] D. Fritter, C. M. Knobler, and D. A. Beysens, Phys. Rev. A **43**, 2858 (1990).
[16] C. M. Knobler and D. Beysens Europhys. Lett. **6**, 707 (1988).
[17] F. Family and P. Meakin, Phys. Rev. Lett. **61**, 428 (1988); M. Klob, *ibid.* **62**, 1699 (1989); F. Family and P. Meakin, *ibid.* **62**, 1700 (1989).
[18] D. Beysens, C. M. Knobler, and H. Schaffar, Phys. Rev. B **41**, 9814 (1990).
[19] T. Aste, M.S. degree thesis, Politecnico di Milano, Milano, 1994.
[20] P. Pozzolini, M.S. degree thesis, University of Genova, Genova, 1994.
[21] F. Saya, M.S. degree thesis, University of Genova, Genova, 1995.
[22] T. Aste, R. Botter, D. Beruto, C. Ciccarelli, M. Giordani, and P. Pozzolini, Sensors Actuators B **18-19**, 637 (1995).
[23] T. Aste, R. Botter, and D. Beruto, Sensors Actuators B **24-25**, 826 (1995).
[24] J. A. Dodds, J. Colloid. Interface Sci. **77**, 317 (1980).
[25] D. Bideau, A. Gervois, L. Oger, and J. P. Troadec, J. Phys. (Paris) **47**, 1697 (1986).
[26] F. Soddy, Nature **137**, 1021 (1936).
[27] H. S. M. Coxeter, Aeq. Math. **1**, 104 (1968).
[28] N. Rivier (private communication).
[29] R. Mosseri and J.-F. Sadoc, in *Geometry in Condensed Matter Physics*, edited by J.-F. Sadoc (World Scientific, Singapore, 1990).
[30] T. Gosset, Nature **139**, 62 (1937).
[31] G. Sberveglieri, G. Faglia, S. Groppelli, P. Nelli, and A. Taroni, Sensors Actuators B **7**, 721 (1992).
[32] P. A. Mulheran (unpublished).
[33] B. Derrida, C. Godreche, and I. Yekutieli, Phys. Rev. A **44**, 6241 (1991).
[34] D. Fritter, C. M. Knobel, D. Roux, and D. Beysens, J. Stat. Phys. **52**, 1447 (1988).

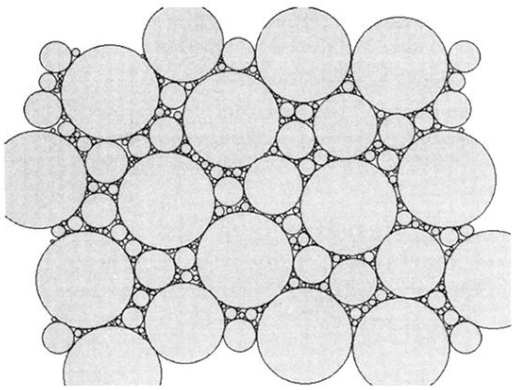

FIG. 2. Computer generated circle covering.

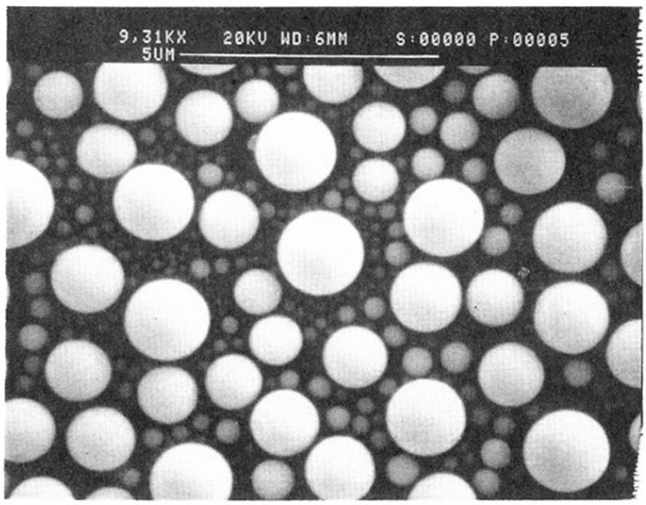

FIG. 4. SEM micrograph of a breath figure generated by tin drops deposited on a hot alumina substrate.